THE JOURNAL OF BIOLOGICAL CHEMISTRY
Vol. 278, No. 11, Issue of March 14, pp. 9212–9218, 2003

Printed in U.S.A.

Rad54p Is a Chromatin Remodeling Enzyme Required for Heteroduplex DNA Joint Formation with Chromatin*

Received for publication, November 12, 2002, and in revised form, January 2, 2003
Published, JBC Papers in Press, January 3, 2003, DOI 10.1074/jbc.M211545200

Mariela Jaskelioff‡§¶, Stephen Van Komen§‖, Jocelyn E. Krebs‡ ‡‡, Patrick Sung‖, and Craig L. Peterson‡§§**

From the ‡Interdisciplinary Graduate Program and Program in Molecular Medicine, University of Massachusetts Medical School, Worcester, Massachusetts 01605, and ‖Department of Molecular Medicine and Institute of Biotechnology, University of Texas Health Science Center at San Antonio, San Antonio, Texas 78245-3207

In eukaryotic cells, the repair of DNA double-strand breaks by homologous recombination requires a RecA-like recombinase, Rad51p, and a Swi2p/Snf2p-like ATPase, Rad54p. Here we find that yeast Rad51p and Rad54p support robust homologous pairing between single-stranded DNA and a chromatin donor. In contrast, bacterial RecA is incapable of catalyzing homologous pairing with a chromatin donor. We also show that Rad54p possesses many of the biochemical properties of *bona fide* ATP-dependent chromatin-remodeling enzymes, such as ySWI/SNF. Rad54p can enhance the accessibility of DNA within nucleosomal arrays, but it does not seem to disrupt nucleosome positioning. Taken together, our results indicate that Rad54p is a chromatin-remodeling enzyme that promotes homologous DNA pairing events within the context of chromatin.

Chromosomal DNA double-strand breaks (DSBs)[1] arise through exposure of cells to harmful environmental agents such as ionizing radiation or mutagenic chemicals (radiomimetics, alkylating agents, etc.). DSBs can also be caused by endogenously produced oxygen radicals, by errors in DNA replication, or as obligatory intermediates during programmed cellular processes, such as meiosis or V(D)J recombination (1–3). Cell survival and maintenance of genome integrity depend on efficient repair of DSBs, because unrepaired or misrepaired DSBs may lead to mutations, gene translocations, gross chromosomal rearrangements, or cellular lethality.

Several pathways for repairing DSBs have evolved and are highly conserved throughout eukaryotes. Homologous recombination (HR) is a major pathway of DSB repair in all eukaryotes and has a distinct advantage over other mechanisms in that it is mostly error-free. In organisms ranging from yeast to human, HR is mediated by members of the *RAD52* epistasis group (*RAD50*, *RAD51*, *RAD52*, *RAD54*, *RAD55*, *RAD57*, *RAD59*, *MRE11*, and *XRS2*). Accordingly, mutations in any one of these genes result in sensitivity to ionizing radiation and other DSB-inducing agents (2). The importance of the HR pathway in maintaining genome integrity is underscored by the fact that mutations in each one of its critical factors have been correlated with chromosomal instability-related ailments, including ataxia telangiectasia-like disease, Nijmegen breakage syndrome, Li Fraumeni syndrome, as well as various forms of cancer (4).

In vivo and *in vitro* studies have suggested the following sequence of molecular events that lead to the recombinational repair of a DSB. First, the 5′ ends of DNA that flank the break are resected by an exonuclease to create ssDNA tails (5). Next, Rad51p polymerizes onto these DNA tails to form a nucleoprotein filament that has the capability to search for a homologous duplex DNA molecule. After DNA homology has been located, the Rad51-ssDNA nucleoprotein filament catalyzes the formation of a heteroduplex DNA joint with the homolog. The process of DNA homology search and DNA joint molecule formation is called "homologous DNA pairing and strand exchange." Subsequent steps entail DNA synthesis to replace the missing information followed by resolution of DNA intermediates to yield two intact duplex DNA molecules (6).

The homologous DNA pairing activity of Rad51p is enhanced by Rad54p (7). Rad54p is a member of the Swi2p/Snf2p protein family (8) that has DNA-stimulated ATPase activity and physically interacts with Rad51p (7, 9, 10). Because of its relatedness to the Swi2p/Snf2p family of ATPases, Rad54p may have chromatin remodeling activities in addition to its established role in facilitating Rad51p-mediated homologous pairing reactions. In this study we show that Rad51p and Rad54p mediate robust D-loop formation with a chromatin donor, whereas the bacterial recombinase, RecA, can only function with naked DNA. Furthermore, we find that the ATPase activity of Rad54p is essential for D-loop formation on chromatin and that Rad54p can use the free energy from ATP hydrolysis to enhance the accessibility of nucleosomal DNA. Experiments are also presented to suggest that chromatin remodeling by Rad54p and yeast SWI/SNF involves DNA translocation.

EXPERIMENTAL PROCEDURES

DNA—All DNA manipulations were carried out using standard methods (11). Oligonucleotides were obtained from Operon Technologies (Alameda, CA). Plasmid pXG540 and T4 EndonucleaseVII used in the cruciform extrusion experiments were a kind gift of Dr. T. Owen-Hughes.

The oligonucleotide used for triplex formation was TFO (triplex-forming oligonucleotide) (5′-TTCTTTTCTTTCTTCTTTCTTT-3′). To

* This work was supported by grants from the National Institutes of Health to C. L. P. (GM49650) and P. S. (GM57814). The costs of publication of this article were defrayed in part by the payment of page charges. This article must therefore be hereby marked "*advertisement*" in accordance with 18 U.S.C. Section 1734 solely to indicate this fact.

§ Both authors contributed equally to this work.

¶ Supported by a U. S. Department of Defense Predoctoral Fellowship (DAMD17-02-1-0471).

** Supported by a U. S. Department of Defense Predoctoral Fellowship (DAMD17-01-1-0414).

‡‡ Current Address: Dept. of Biological Sciences, University of Alaska, 3211 Providence Dr., Anchorage, AK 99508.

§§ To whom correspondence should be addressed. Tel.: 508-856-5858; Fax: 508-856-5011; E-mail: Craig.Peterson@umassmed.edu.

[1] The abbreviations used are: DSB, double-strand break; HR, homologous recombination; ssDNA, single-stranded DNA; dsDNA, double-stranded DNA; TFO, triplex-forming oligonucleotide; DTT, dithiothreitol; BSA, bovine serum albumin; ATPγS, adenosine 5′-*O*-(thiotriphosphate); AMP-PNP, adenosine 5′-(β,γ-imino)triphosphate; Mnase, micrococcal nuclease.

generate pMJ5, the annealed oligonucleotides TFOB5 (5′-TCGAGAAGAAAAGAAAGAAGAAAGAAAC-3′) and TFOB3 (5′-TCGAGT TTCTTTCTTTCTTTTCTTC-3′) were ligated to the product of a *Xho*I digestion carried out on pCL7c (12). This yielded a pBluescript SKII (−) plasmid containing 5 head-to-tail repeats of the 208-bp *Lytechinus variegatus* 5S rDNA nucleosome positioning element flanked by a TFO-binding site. The DNA template (208–11) for reconstituting nucleosomal arrays for the ATPase, remodeling, and Mnase assays consists a *Not*I-*Hin*dIII fragment derived from pCL7b (12), containing 11 head-to-tail repeats of a 5S rRNA gene from *L. variegatus*, each one possessing a nucleosome positioning sequence. The sixth nucleosome is tagged by a unique *Sal*I restriction site.

Reagent Preparation—Recombinant yeast Rad51p, Rad54p, rad54K341Ap, and rad54K341Rp were overexpressed in yeast and purified as previously described (7). SWI/SNF purification was as described (13). Histone octamers were purified from chicken erythrocytes as described by Hansen *et al.* (14). Octamer concentrations were determined by measurements of A_{230} (15). Nucleosomal array DNA templates (pXG540, pMJ5, or 208–11) were labeled by the Klenow polymerase fill-in reaction using [α-^{32}P]dCTP (3000 μCi/mmol, Amersham Biosciences). Nucleosomal arrays were reconstituted by salt dialysis as previously described (13), and the nucleosome saturation was determined to be 60–80% by digestion analysis.

D-loop Reactions—Oligonucleotide D1 (90-mer) used in the D-loop experiments has the sequence: 5′-AAATCAATCTAAAGTATATATGAGTAAACTTGGTCTGACAGTTACCAATGCTTAATCAGTGAGGCACCTATCTCAGCGATCTGTCTATTT-3′, being complementary to positions 1932–2022 of pBluescript SK(−) replicative form I DNA. Oligonucleotide D1 was 5′ end-labeled with ^{32}P using [γ-^{32}P]dATP and polynucleotide kinase, as described (7). Buffer R (35 mM Tris-HCl, pH 7.4, 2.0 mM ATP, 2.5 mM $MgCl_2$, 30 mM KCl, 1 mM DTT, and an ATP-regenerating system consisting of 20 mM creatine phosphate and 30 μg/ml creatine kinase) was used for the reactions; all of the incubation steps were carried out at 30 °C. Rad51 (0.8 μM) and Rad54 (120 nM) were incubated with radiolabeled oligonucleotide D1 (2.4 μM nucleotides) for 5 min to assemble the presynaptic filament, which was then mixed with naked pBluescript replicative form I DNA (38 μM base pairs) or the same DNA assembled into chromatin (38 μM base pairs). Chromatin assembly was monitored by following topological changes as well as measuring the degree of occlusion of a unique *Eco*RI restriction site close to the D1 sequence. Substrates were estimated to be ~80% saturated with nucleosomes. The reactions containing RecA protein (0.8 μM) were assembled in the same manner, except that they were supplemented with an additional 12.5 mM $MgCl_2$ at the time of incorporation of the duplex substrates. At the indicated times, 4-μl portions of the reactions were withdrawn and mixed with an equal volume of 1% SDS containing 1 mg/ml proteinase K. After incubation at 37 °C for 5 min, the deproteinized samples were run in 1% agarose gels in TAE buffer (40 mM Tris-HCl, pH 7.4, 0.5 mM EDTA) at 4 °C. The gels were dried, and the radiolabeled DNA species were visualized and quantified by PhosphorImager analysis (Personal Molecular Imager FX, Bio-Rad).

ATPase Assay—Recombinant yeast Rad54p (1 nM) was incubated at 30 °C or 37 °C with 5 nM of either naked 208–11 dsDNA or reconstituted nucleosomal arrays in the presence of 100 μM ATP, 2.5μCi [γ-^{32}P]dATP (6000 μCi/mmol, Amersham Biosciences), 2.5% glycerol, 0.1% Tween 20, 20 mM Tris-HCl, pH 8.0, 200 μM DTT, 5 mM $MgCl_2$, 100 μg/ml BSA. For the DNA length-dependence assays, 5 nM Rad54p, 5 nM Rad51p, or 10 nM SWI/SNF were used. Oligonucleotides (random N-mers ranging from 10–100 nucleotides in length) were PAGE-purified to ensure length homogeneity (Integrated DNA Technologies, Inc., Coralville, IA). Samples were taken after 2, 5, 15, and 30 min and resolved by TLC. The proportion of liberated ^{32}P-pyrophosphate was determined using the Molecular Dynamics PhosphorImager and ImageQuant Software. ATPase assays were independently repeated 3 times, yielding very similar results.

Cruciform Formation Assay—Cruciform formation assays were performed as previously described (16). Briefly, 8 ng of *Ava*I-linearized pXG540 (either naked, N, or nucleosomal, C) were incubated with various concentrations of Rad54, Rad51, or rad54 K341A and 0.15 mg/ml EndoVII (except where noted), in the presence of 10 mM Hepes, pH 7.9, 50 mM NaCl, 3 mM $MgCl_2$, 5% glycerol, 0.1 mM DTT, 1 mM ATP (except where noted), 3 mM phosphoenolpyruvate, and 20 units/ml pyruvate kinase for 30 min at 30 °C. The products were resolved in 1.2% agarose gels and visualized with Sybr Gold staining (Molecular Probes, Eugene, OR) followed by analysis with ImageQuant software.

Chromatin-remodeling Reaction—For the coupled SWI/SNF-or Rad54-*Sal*I reactions, reconstituted 208–11 nucleosomal arrays (~1 nM final concentration) were preincubated at 37 °C for 20 min with 2.5units/μl *Sal*I in a buffer containing (final concentrations) 50 mM NaCl, 5 mM $MgCl_2$, 1 mM ATP, 3 mM phosphoenolpyruvate, 10 units/ml pyruvate kinase, 1 mM DTT, 10 mM Tris-HCl, pH 8.0, 100 μg/ml BSA, and 3% glycerol. Nucleosomal arrays were ~80% saturated with nucleosomes. Buffer, 2 nM SWI/SNF complex, or various concentrations of recombinant Rad51p and Rad54p were added and samples were taken at the indicated time points, vigorously mixed for 10s with 25 μl TE and 50 μl 1:1 solution of phenol/chloroform. The purified DNA fragments were resolved by electrophoresis in 1.2% agarose gels in the presence of 50 μg/ml ethidium bromide. The gels were then dried on 3MM Whatman paper. The fraction of cut and uncut DNA was determined by PhosphorImager analysis using a Molecular Dynamics PhosphorImager and ImageQuant software. Experiments were repeated independently at least 3 times, which yielded very similar results.

Micrococcal Nuclease Digestion—15 nM reconstituted 208–11 nucleosomal arrays were incubated at 37 °C with 2 nM SWI/SNF, 100 nM Rad54p, or buffer, in the presence of 2 mM ATP, 5 mM NaCl, 2.5 mM Tris-HCl, pH 8.0, 0.25 mM $MgCl_2$, 0.3 mM $CaCl_2$, 3 mM phosphoenolpyruvate, 10 units/ml pyruvate kinase, 1 mM DTT, 10 μg/ml BSA, 0.5% glycerol. After 20 min, 0.0005 units of Micrococcal Nuclease (Worthington) was added to the reaction, and aliquots were taken at the indicated time points and then treated for 20 min with 2 μg/μl proteinase K and extracted twice with a 1:1 solution of phenol:chloroform. The resulting digestion products were resolved by electrophoresis in 2% agarose gels, run at 2.5 volts/cm for 12 h. The gels were fixed, dried, and analyzed using a Molecular Dynamics PhosphorImager and ImageQuant Software.

Triple-helix Displacement Assay—Triple-helix formation was performed as described (17). Briefly, equimolar concentrations (100 nM) of *Ssp*I-linearized pMJ5 and ^{32}P-labeled TFO were mixed in buffer MM (25 mM MES, pH 5.5, 10 mM $MgCl_2$) at 57 °C for 15 min and left to cool to room temperature overnight. The resulting triplex was either used directly or reconstituted into nucleosomal arrays. To introduce nicks into the DNA, pMJ5 was exposed to various concentrations of DNaseI (Promega, Madison, WI) for 2 min at 37 °C, the reactions were stopped with 5 mM EDTA, vigorously mixed for 10 s with a 1:1 solution of phenol/chloroform, ethanol-precipitated, and resuspended in water. The degree of nicking introduced by DNaseI treatment was assessed by electrophoretic analysis of native and heat-denatured samples (in the presence of 15% formamide) on denaturing 1.3% agarose gels, followed by Sybr Gold Stain (Molecular Probes, Eugene, OR).

The triplex-containing substrates (5 nM) were incubated at 30 °C with 5 nM recombinant Rad54 protein or SWI/SNF complex, in a buffer containing 35 mM Tris-HCl, pH 7.2, 3 mM $MgCl_2$, 100 μg/ml BSA, 50 mM KCl, 1 mM DTT, 3 mM phosphocreatine, 28 μg/ml creatine phosphokinase, and where noted, 3 mM ATP. Samples were taken at the indicated time points, the reactions were quenched with GSMB buffer (15% (w/v) glucose, 3% (w/v) SDS, 250 mM 4-morpholinepropanesulfonic acid, pH 5.5, 0.4 mg/ml bromphenol blue), and analyzed in 1.2% agarose gels (40 mM Tris acetate, 5 mM sodium acetate, 1 mM $MgCl_2$, pH 5.5) at 10 volts/cm for 1.5 h at 4 °C. Gels were fixed in 5% acetic acid, 50% methanol for 1 h, and dried. The proportion of bound and free TFO was determined using a Molecular Dynamics PhosphorImager and ImageQuant Software.

RESULTS

Rad51p and Rad54p Promote DNA Pairing with a Chromatin Donor—Repair of a DSB by homologous recombination begins with the invasion of a double-stranded, homologous donor by a Rad51-ssDNA nucleoprotein filament, also referred to as the presynaptic filament. This strand invasion reaction is typically monitored *in vitro* by following the Rad51p-dependent formation of a D-loop between a radiolabeled oligonucleotide and a homologous double-stranded DNA donor (Fig. 1*A*). In this case, efficient D-loop formation also requires the ATPase activity of Rad54p. *In vivo*, however, the search for homology and strand invasion involves a homologous donor that is assembled into chromatin. Given that the Rad54p ATPase shows sequence relatedness to known chromatin remodeling enzymes, it was of considerable interest to examine the ability of Rad54p to promote Rad51p-dependent D-loop formation with a nucleosomal donor.

Fig. 1 shows the results of D-loop assays that use either a circular, naked DNA donor or this same circular DNA assembled into nucleosomes. Consistent with previous studies, the

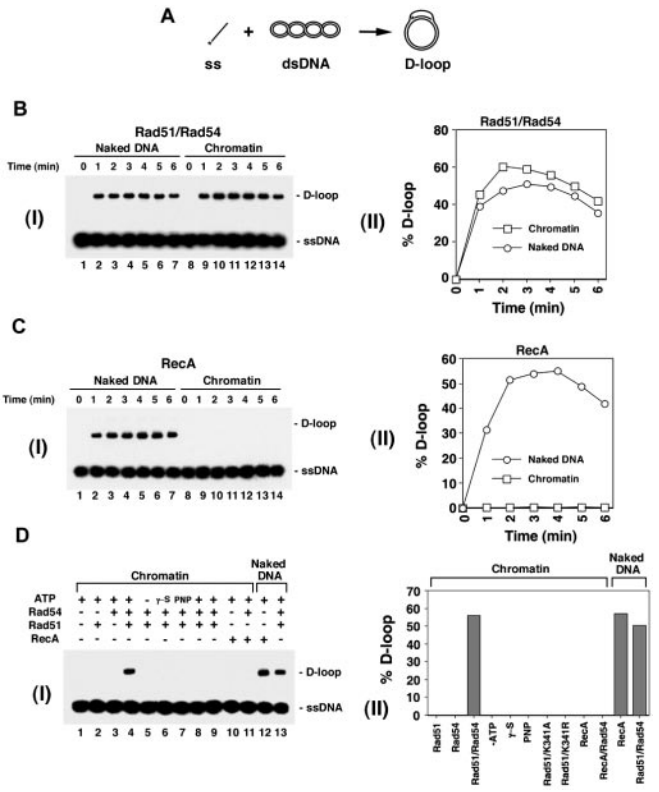

FIG. 1. **Rad51p and Rad54p promote efficient DNA strand invasion with chromatin.** *A*, schematic of the D-loop reaction. A radiolabeled oligonucleotide (*ss*) pairs with a homologous duplex target (*dsDNA*) to yield a D-loop, which, after separation from the free oligonucleotide on an agarose gel, is visualized and quantified by PhosphorImager analysis of the dried gel. *B*, *panel I* shows D-loop reactions mediated by Rad51p and Rad54p with the naked homologous duplex (*Naked DNA*) and the homologous duplex assembled into chromatin (*Chromatin*). The results from the experiments in *panel I* are graphed in *panel II*. The *ordinate* refers to the proportion of the homologous duplex converted into D-loop. *C*, *panel I* shows D-loop reactions mediated by RecA with the naked homologous duplex (*Naked DNA*) and the homologous duplex assembled into chromatin (*Chromatin*). The results from the experiments in *panel I* are graphed in *panel II*. *D*, *panel I* shows D-loop reactions in which Rad51p and RecA were used either alone or in conjunction with Rad54p or rad54 mutant variants with the naked homologous duplex (*Naked DNA*) and the homologous duplex assembled into chromatin (*Chromatin*), as indicated. ATP was omitted from the reaction in *lane 5*, and ATPγS (*γS*) and AMP-PNP (*PNP*) replaced ATP in *lanes 6* and *7*, respectively. The reactions in *lanes 8* and *9* contained ATP, but Rad54p was replaced with the ATPase-defective variants rad54 K341A (*KA*) and rad54 K341R (*KR*), respectively. The results from the experiments in *panel I* are summarized in the bar graph in *panel II*.

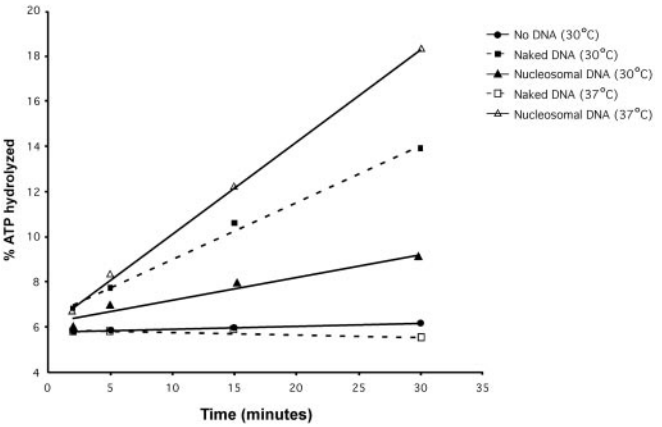

FIG. 2. **Nucleosomal DNA protects Rad54p from thermal inactivation.** ATPase assays. 1 nM Rad54p was incubated at 30 °C with no DNA (*circles*), 5 nM naked (*closed squares*) or nucleosomal dsDNA (*closed triangles*), or at 37 °C with 5 nM naked (*open squares*) or nucleosomal dsDNA (*open triangles*). Samples were taken after 2, 5, 15, and 30 min.

combination of yeast Rad51p and Rad54p led to rapid and highly efficient D-loop formation on the naked DNA donor (Fig. 1*B*). A similar level of D-loop formation was also obtained when the bacterial recombinase RecA was used in these assays with naked DNA (Fig. 1*C*). Surprisingly, assembly of the circular donor into chromatin had no effect on the efficiency of D-loop formation by Rad51p and Rad54p (Fig. 1*B*). D-loop formation on the chromatin donor required ATP hydrolysis by Rad54p, because nonhydrolyzable ATP analogs (ATPγS and AMP-PNP) were unable to substitute for ATP (Fig. 1*C*, *panel I*, *lanes 6* and *7*), and two ATPase-defective mutant variants of Rad54p, rad54K341Ap and rad54K341Rp (18), were inactive (Fig. 1*D*). In contrast to reactions that contained Rad51p/Rad54p, the activity of RecA was completely eliminated when the donor was assembled into nucleosomes (Fig. 1*C*). Furthermore, addition of Rad54p to the RecA reaction did not rescue D-loop formation on chromatin (Fig. 1*D*, *panel I*, *lane 11*). Thus, the eukaryotic recombination proteins have the unique capability of performing the DNA strand invasion reaction with a chromatin donor.

Nucleosomal DNA Protects Rad54p from Thermal Denaturation—The ATPase activity of Rad54p is required for many of its biological functions *in vivo* and for enhancing Rad51p-mediated homologous DNA pairing reactions *in vitro*, both on naked DNA (18) and on chromatin (Fig. 1*D*). Given the latter finding, we were interested in determining whether chromatin influences the ATPase activity of Rad54p.

As shown in Fig. 2, both naked DNA (*solid squares*) and chromatin (*solid triangles*) stimulated the ATPase activity of Rad54p at 30 °C, with naked DNA being somewhat more effective. At the low protein concentrations at which these assays were performed (1 nM), purified Rad54p is extremely temperature-labile and is rapidly inactivated at 37 °C (Fig. 2; Ref. 36). Thus, as expected, the ATPase activity of Rad54p was not detectable in the presence of naked DNA when the reactions were performed at 37 °C (Fig. 2, *open squares*). Importantly, when the reaction was carried out in the presence of chromatin (*open triangles*), the rate of ATP hydrolysis at 37 °C was even greater than the rate obtained in reactions conducted at 30 °C. Importantly, there was no measurable ATPase activity associated with the nucleosomal arrays in the absence of Rad54p, and BSA, free histones, and replication protein A were unable to stimulate the DNA-stimulated ATPase activity of Rad54p at 37 °C. These results indicate that nucleosomal DNA is uniquely able to protect Rad54p from thermal inactivation, and these data suggest that Rad54p may physically interact with nucleosomes.

Rad54 Generates Unconstrained Superhelical Torsion in Nucleosomal DNA—A number of chromatin remodeling complexes that contain Swi2/Snf2-related ATPases have been shown to alter chromatin structure by generating superhelical torsion in DNA and nucleosomal arrays (16). Indeed, the ability to introduce superhelical stress may represent a primary biomechanical activity of all Swi2/Snf2-like ATP-dependent DNA motors, and this activity is likely to be crucial for catalyzing alterations in chromatin structure. Previous studies have shown that Rad54p can also generate both negative and positive supercoiled domains in dsDNA, and it has been suggested that this activity reflects the tracking of Rad54p along DNA (19, 20).

We investigated whether Rad54p is able to introduce superhelical torsion on nucleosomal substrates, using a cruciform extrusion test that has been used for examining other chromatin remodeling enzymes (Fig. 3*A*). In this assay, superhelical

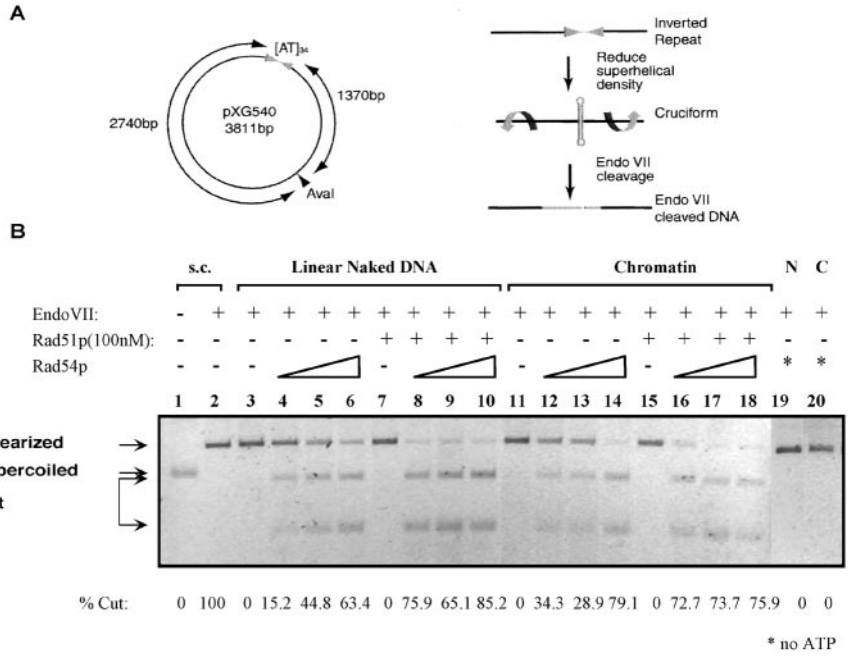

FIG. 3. **Rad54 generates superhelical torsion on nucleosomal DNA.** *A*, schematic illustration of the cruciform extrusion assay. A linearized plasmid (*pXG540*) containing an inverted repeat sequence is incubated with T4 Endonuclease VII, a highly selective junction resolving enzyme, and Rad54p, in the presence of ATP. Rad54p increases the local unconstrained superhelical density, resulting in the extrusion of a cruciform structure, which is recognized and cut by Endo VII. Adapted from Havas *et al.* (16). *B*, results of a typical cruciform formation assay. Supercoiled (*lanes 1*, *2*), *Ava*I-linearized pXG540 DNA (*lanes 3–10*, *19*), or nucleosomal pXG540 (*lanes 11–18*, *20*) was incubated with 12.5, 25, or 50 nM Rad54p as indicated, in the presence or absence of 100 nM Rad51p. EndoVII was omitted in *lane 1*. ATP was omitted in *lanes 19* and *20*. The numbers below each lane (*% cut*) represent the percentage of pXG540 molecules cleaved by EndoVII. *s.c.*, supercoiled substrate; *C*, chromatin substrate; *N*, naked linear DNA substrate.

torsion leads to extrusion of a cruciform that is then recognized and cleaved by bacteriophage T4 endonuclease VII that has high specificity for this DNA structure (16). Consistent with previous studies (19), Rad54p action generates torsional stress on a linear, dsDNA substrate (*N*) which leads to cruciform extrusion (Fig. 3*B*, *lanes 4–6*). Importantly, Rad54p was able to generate torsional stress on the nucleosomal substrate (*C*) with comparable efficiency (*lanes 12–14*). The addition of 100 nM Rad51p greatly stimulated the ability of Rad54p to promote the formation of cruciform structures on both naked and nucleosomal substrates (compare *lanes 4* and *8*, and *12* and *16*, respectively. Also note the decreased levels of linear template in *lanes 16–18*). Importantly, Rad51p fails to support cruciform formation by itself (*lanes 7* and *15*). As expected, the generation of torsional stress required ATP (*lanes 19* and *20*). Furthermore, the ATP hydrolysis mutant variant rad54 K341A was inactive in these assays (data not shown). These data indicate that Rad54p, like other Swi2/Snf2 family members, uses the free energy from ATP hydrolysis to alter DNA topology and that nucleosomal arrays constitute excellent substrates for this activity.

Rad54p Can Disrupt a DNA Triple Helix—How Rad54p introduces topological stress in nucleosomal DNA is unclear. Previously, we suggested that superhelical torsion might result from translocation of Rad54p along the DNA double helix (19). Recently, chromatin remodeling by the yeast RSC complex (which contains the Swi2/Snf2-related ATPase, Sth1p) has been shown to involve ATP-dependent DNA translocation (21). To further evaluate the ability of Rad54p to translocate on DNA, we used a DNA triple-helix-displacement assay that was originally developed to follow the translocation of a type I restriction endonuclease along DNA (17). The substrate used (see Fig. 4*A*) consists of a radioactively labeled oligonucleotide (TFO*) bound via Hoogsteen hydrogen bonds to the major groove of a 2.5-kb linear dsDNA. Translocation of a protein along the DNA displaces the triplex, which can be detected as dissociation of the radioactive TFO* from the DNA triplex. Fig. 4*B* shows typical levels of triplex displacement in the absence or presence of Rad54p or yeast SWI/SNF. Both Rad54p and ySWI/SNF were able to efficiently displace a preformed triplex from both naked (*squares*) and nucleosomal (*triangles*) substrates in an ATP-dependent manner. Similar results were

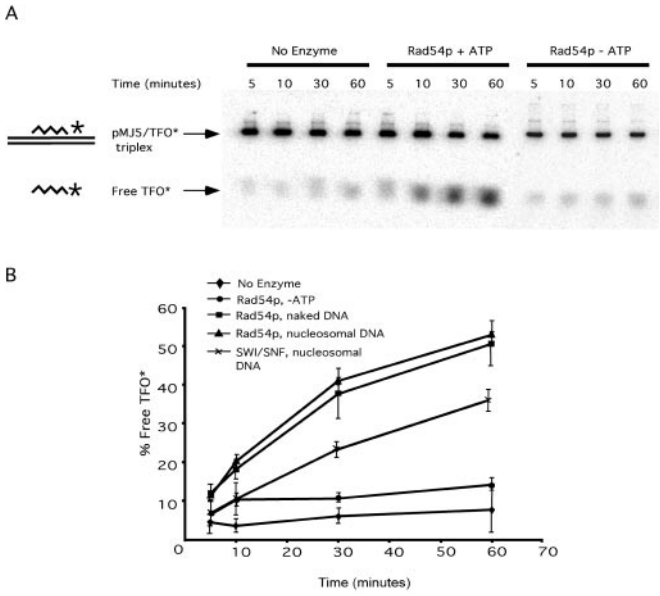

FIG. 4. **Rad54p action displaces a preformed triplex.** *A*, typical results obtained with naked triplex-containing substrate. The upper band corresponds to the duplex-bound TFO*; the lower band corresponds to free TFO*. Reactions contained 5 nM triplex substrate and 5 nM Rad54p. *B*, percentage of free TFO* in four or more experiments were averaged and plotted as a function of time. Note that triplex displacement from the nucleosomal template occurs at equal efficiency to that of naked DNA.

obtained when the TFO*-bound substrate contained single-strand nicks (data not shown), strongly suggesting that the displacement of the TFO* reflects translocation of Rad54p and ySWI/SNF and that it is not due simply to the generation of torsional stress. Thus, yeast RSC (21), ySWI/SNF, and Rad54p (Fig. 4) all share the ability to use the free energy from ATP hydrolysis to disrupt triplex DNA.

Rad54p Has ATPase Kinetics Diagnostic of a DNA-translocating Enzyme—The "inch-worm" model for DNA translocation, originally envisioned (22) for DNA helicases and later modified by Velankar *et al.* (23), proposes that the translocating enzyme progresses along the contour of the DNA in steps of

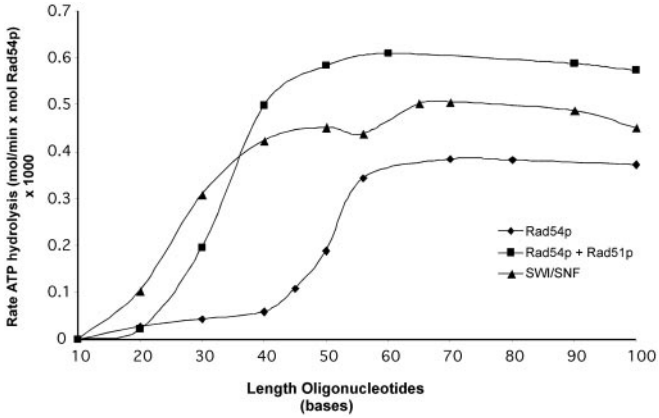

FIG. 5. **Rad54 has ATPase kinetics typical of a unidirectional DNA translocating enzyme.** The rate of ATP hydrolysis by 5 nM Rad54p (*diamonds*), 5 nM Rad54p + 5 nM Rad51p (*squares*), or 10 nM SWI/SNF (*triangles*) was measured in the presence of 50 μM ssDNA (n-mers) oligonucleotides of different lengths. The average values from 3 independent experiments were plotted. Rates were determined from experiments with at least four time points.

a single base, and each step requires the hydrolysis of one ATP molecule. This model predicts that the rate of ATP hydrolysis of a unidirectional DNA translocating enzyme will depend on the length of the DNA (24).

To investigate whether Rad54p has ATPase properties characteristic of a unidirectional DNA translocating enzyme, the rate of ATP hydrolysis was measured in the presence of saturating amounts of single-stranded oligonucleotides ranging from 10 to 100 nucleotides in length (Fig. 5). For comparison, we also monitored the ATPase activity of yeast SWI/SNF (*triangles*). In the case of Rad54p, oligonucleotides shorter than 40 bases failed to stimulate the ATPase activity of Rad54p (*diamonds*), whereas oligonucleotides between 40 and 70 bases led to a stimulation of ATPase activity that was proportional to DNA length. For oligonucleotides longer than 70 bases, the ATPase activity no longer increased with the DNA length. When Rad51p was added to these reactions (*squares*), shorter oligonucleotides became more effective in promoting ATP hydrolysis, and the overall activity was enhanced. Likewise, the ATPase activity of ySWI/SNF (*triangles*) was also proportional to the DNA length, with a plateau reached at 60 bases.

These results are fully consistent with both Rad54p and ySWI/SNF coupling ATP hydrolysis to unidirectional translocation, in which the rate of DNA binding is slower than the rate of DNA translocation (21). In this case, no ATP hydrolysis is observed with very short substrates, presumably because a minimum DNA length is required for Rad54p or ySWI/SNF to bind and to translocate before reaching an end and releasing the DNA. When the substrate is ~30–40 nucleotides in length, Rad54p and ySWI/SNF readily bind the substrate, and more extended translocation events take place. The rate of ATP hydrolysis is fairly constant with DNA substrates longer than 60–70 nucleotides, reflecting the possibility that Rad54p and ySWI/SNF have little processivity, and thus they release their substrate after ~60–70 bases regardless of the total length of the DNA molecule. Although the triphasic kinetics of ATPase activity are consistent with a DNA-translocation mechanism, it remains a possibility that the longer single-stranded oligonucleotides exhibit more extended secondary structures that are either more proficient at binding Rad54p (or SWI/SNF) or stimulating its ATPase activity.

Rad54 Is an ATP-dependent Chromatin Remodeling Enzyme—Cairns and colleagues (21) proposed that short-range translocation events may be the key feature of chromatin remodeling enzymes, leading to a "pumping" of DNA across the surface of the histone octamer, which then results in enhanced DNA accessibility and nucleosome movements. To investigate whether Rad54p might also enhance the accessibility of nucleosomal DNA, we used an assay in which nucleosome remodeling activity is coupled to restriction enzyme activity such that remodeling is revealed as an enhancement of restriction-enzyme cleavage rates (12). This assay uses a nucleosomal array substrate in which the central nucleosome of an 11-mer array contains a unique *Sal*I site located at the predicted dyad axis of symmetry (see Fig. 6*A*). In the absence of a remodeling enzyme, the rate of *Sal*I cleavage is very slow (Fig. 6*A*, *solid diamonds*), whereas addition of a remodeling enzyme, such as yeast SWI/SNF, leads to enhanced digestion (Fig. 6*A*, *solid squares*). When Rad54p was added to the remodeling reactions, *Sal*I digestion was also dramatically enhanced (*solid circles*, *triangles*), although a higher concentration of this protein (50 nM) was required to achieve a rate of digestion comparable with that of reactions that contained yeast SWI/SNF (2 nM, *squares*). However, when Rad51p (50 nM) and Rad54p (50 nM) were both present in the reaction, much higher levels of remodeling were attained (*open circles*). Note that Rad51p has no intrinsic chromatin remodeling activity (*open diamonds*). The stimulation of the Rad54p chromatin remodeling activity by Rad51p is congruent with previous studies showing that Rad51p enhances the rate of ATP hydrolysis and DNA supercoiling by Rad54p (19, 25, see Fig. 3). Thus, the above data indicate that Rad54p is sufficient for chromatin remodeling activity but that the combination of Rad51p and Rad54p constitutes a more potent remodeling machine.

Rad54p Does Not Induce Significant Nucleosome Mobilization—A number of chromatin remodeling complexes that contain a Swi2/Snf2-related ATPase (ySWI/SNF, dCHRAC, dNURF, and xMi-2) can use the energy of ATP hydrolysis to move nucleosomes in cis (26–30). To investigate whether Rad54p can also catalyze nucleosome mobilization, ^{32}P-end-labeled nucleosomal arrays were incubated with buffer, ySWI/SNF, or Rad54p, and nucleosome positions were mapped by micrococcal nuclease (Mnase) digestion (Fig. 6*B*). Mnase can only cleave DNA between nucleosomes, which leads to a periodic ladder of digestion products indicative of a positioned 11-mer nucleosomal array (Fig. 6*B*). Consistent with our previous studies, incubation with ySWI/SNF (2 nM) and ATP leads to a complete disruption of the Mnase digestion pattern, indicative of nucleosome sliding (Fig. 6*B*, *left panel*; also see Ref. 28). In contrast, addition of Rad54p (100 nM) and ATP had very little effect on the cleavage periodicity (Fig. 6*B*, *right panel*). Likewise, addition of both Rad51p and Rad54p (100 nM each) to these assays did not change the Mnase digestion profile (data not shown). Importantly, these experiments used concentrations of ySWI/SNF and Rad54p that yielded similar levels of chromatin remodeling in the restriction enzyme accessibility assay (Fig. 6*A*). Thus, although Rad54p can enhance the accessibility of nucleosomal DNA to restriction enzymes, this activity does not appear to reflect large scale rearrangement of nucleosome positions.

DISCUSSION

In eukaryotes, chromatin presents an accessibility dilemma for all DNA-mediated processes, including gene transcription and DNA repair. Although much progress has been made on identifying the enzymes that remodel chromatin structure to facilitate transcription, less is known of how the DNA-repair machinery gains access to damaged DNA within chromatin (reviewed in Ref. 31). In particular, it has not been clear how the recombinational repair machinery can locate short regions of DNA homology when those DNA donor sequences are assembled into chromatin. Here we have shown that the yeast re-

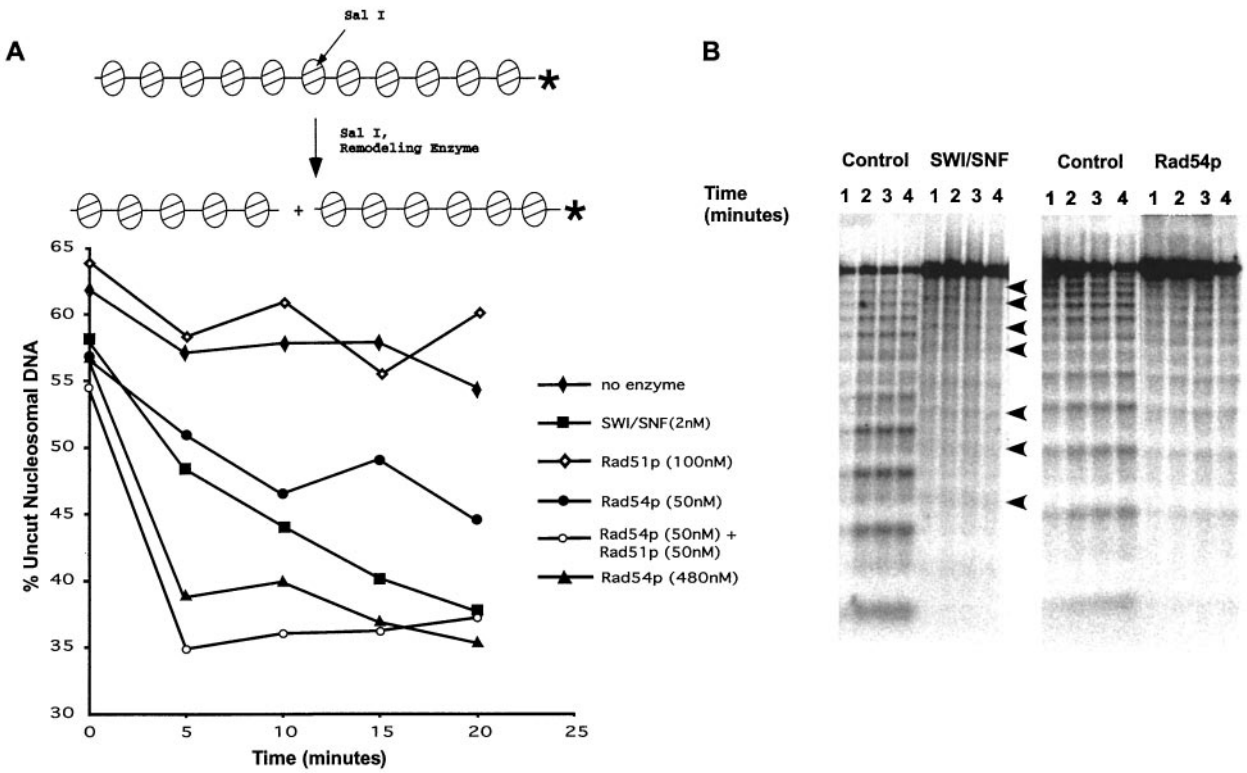

FIG. 6. **Rad54 is an ATP-dependent chromatin remodeling enzyme.** *A*, various concentrations of recombinant Rad54p were tested for chromatin-remodeling activity in a coupled remodeling-restriction enzyme cleavage assay. The nucleosomal substrate was incubated with 50 nM (*closed circles*) or 480 nM Rad54p (*triangles*), 100 nM Rad51p (*open diamonds*), 50 nM Rad54p + 50 nM Rad51p (*open circles*), 2 nM ySWI/SNF (*squares*), or buffer (*closed diamonds*). *B*, 208–11 reconstituted nucleosomal arrays were incubated at 37 °C with 2 nM SWI/SNF, 100 nM Rad54p, or buffer (control lanes). Aliquots were treated with Mnase for the indicated times. The *arrowheads* in the *left panel* indicate the alternate banding pattern as a result of SWI/SNF-induced nucleosome movement.

combination proteins, Rad51p and Rad54p, are sufficient to promote heteroduplex DNA joint formation with chromatin. In contrast, the bacterial recombinase RecA is completely inactive with a chromatin donor. The unique capacity of the eukaryotic machinery to contend with chromatin likely reflects the chromatin-remodeling activity of Rad54p, in which the free energy from ATP hydrolysis enhances the accessibility of nucleosomal DNA. Strand invasion with chromatin may also require a specific interaction between Rad51p and Rad54p because the chromatin remodeling activity of Rad54p does not facilitate RecA-dependent D-loop formation with chromatin (Fig. 1*D*). Recently, Alexiadis and Kadonaga have reported that the *Drosophila* Rad51 and Rad54 proteins can also facilitate strand invasion with chromatin (35).

How Does Rad54p Remodel Chromatin Structure?—Several studies have shown that SWI/SNF-like chromatin remodeling enzymes can perform two separable reactions: 1) they can use the free energy from ATP hydrolysis to enhance the accessibility of nucleosomal DNA and 2) they can use this free energy to mobilize nucleosomes in cis (reviewed in Ref. 32). Recent work from Cairns and colleagues have suggested that both of these activities may be caused by ATP-dependent "pumping" of DNA into the nucleosome (21). In this model, small amounts of DNA translocation might lead to transient exposure of small "loops" of DNA on the surface of the histone octamer, whereas larger quantities of DNA "pumped" into the nucleosome would lead to changes in nucleosome positions. Our data support this model, as we find that both yeast SWI/SNF and Rad54p, like yeast RSC (21), can disrupt a DNA triplex in an ATP-dependent reaction, presumably by translocation of DNA along the surface of the enzyme or by translocation of the enzyme along the DNA. Furthermore, the ATPase activities of ySWI/SNF and Rad54p are sensitive to DNA length, which is diagnostic of DNA-translocating enzymes (21).

Although ySWI/SNF and Rad54p can both enhance the accessibility of nucleosomal DNA, only ySWI/SNF appears to be proficient at changing nucleosome positioning. This result suggests that the precise mechanism of chromatin remodeling by Rad54p may be distinct from that of ySWI/SNF. For instance, Rad54p may only be able to pump small amounts of DNA across the histone octamer surface. Alternatively, Rad54p may translocate along DNA, rather than pumping DNA into the nucleosome. In this model, Rad54p may "pull" the Rad51-ssDNA nucleoprotein filament along the chromatin fiber, leading to changes in nucleosomal DNA topology and DNA accessibility. Such a DNA tracking mechanism might play a key role in facilitating both the search for homology as well as the strand invasion step.

Multiple Roles for Rad54p during Homologous Recombination—Our results suggest that Rad54p is an extremely versatile recombination protein that plays key roles in several steps of homologous recombination. Recently, we found that Rad54p is required for optimal recruitment of Rad51p to a double strand break *in vivo*, and likewise Rad54p can promote formation of the presynaptic filament *in vitro* by helping Rad51p contend with the inhibitory effects of the ssDNA-binding protein replication protein A.[2] Several studies over the past few years have also shown that the ATPase activity of Rad54p plays key roles subsequent to formation of the presynaptic filament. For instance, Rad54p is required for the Rad51p-nucleoprotein filament to form a heteroduplex joint DNA mol-

[2] B. Wolner, S. Van Komen, P. Sung, and C.L. Peterson, submitted for publication.

ecule, even when the homologous donor is naked DNA (Fig. 1*A*; see also Refs. 7, 18, 33). In this case, it has been proposed that Rad54p might use the free energy from ATP hydrolysis to translocate along DNA, which facilitates the homology search process. This DNA-translocation model is fully consistent with our findings that Rad54p can displace a DNA triplex and that the ATPase activity of Rad54p is proportional to DNA length. Rad54p also stimulates heteroduplex DNA extension of established joint molecules (34). Finally, we have shown that Rad54p is required for Rad51p-dependent heteroduplex joint molecule formation with a chromatin donor. In this case, our results suggest that the ATPase activity of Rad54p is used to translocate the enzyme along the nucleosomal fiber, generating superhelical torsion, which leads to enhanced nucleosomal DNA accessibility. It seems likely that this chromatin remodeling activity of Rad54p might also facilitate additional steps after heteroduplex joint formation. Future studies are now poised to reconstitute the complete homologous recombinational repair reaction that fully mimics each step in the repair of chromosomal DNA double strand breaks *in vivo*.

REFERENCES

1. Hiom, K. (2001) *Curr. Biol.* **11,** R278–R280
2. Pâques, F., and Haber, J. E. (1999) *Microbiol. Mol. Biol. Rev.* **63,** 349–404
3. Wood, R. D., Mitchell, M., Sgouros, J., and Lindhal, T. (2001) *Science* **291,** 1284–1289
4. Khanna, K. K., and Jackson, S. P. (2001) *Nat. Genet.* **27,** 247–254
5. Melo, J., and Toczyski, D. (2002) *Curr. Opin. Cell Biol.* **14,** 237–245
6. Kanaar, R., Hoeijmakers, J. H. J., and van Gent, D. C. (1998) *Trends Cell Biol.* **8,** 483–489
7. Petukhova, G., Stratton, S., and Sung, P. (1998) *Nature* **393,** 91–94
8. Eisen, J. A., Sweder, K. S., and Hanawalt, P. C. (1995) *Nucleic Acids Res.* **23,** 2715–2723
9. Jiang, H., Xie, Y., Houston, P., Stemke-Hale, K., Mortensen, U. H., Rothstein, R., and Kodadek, T. (1996) *J. Biol. Chem.* **271,** 33181–33186
10. Clever, B., Interthal, H., Schmuckli-Maurer, J., King, J., Sigrist, M., and Heyer, W. D. (1997) *EMBO J.* **16,** 2535–2544
11. Sambrook, J., Fritsch, E. F., and Maniatis, T. (1989) *Molecular Cloning: A Laboratory Manual*, Cold Spring Harbor Laboratory, Cold Spring Harbor, NY
12. Logie, C., and Peterson, C. L. (1997) *EMBO J.* **16,** 6772–6782
13. Logie, C., and Peterson, C. L. (1999) *Methods Enzymol.* **304,** 726–741
14. Hansen, J. C., Ausio, J., Stanik, V. H., and van Holde, K. E. (1989) *Biochemistry* **28,** 9129–9136
15. Stein, A. (1979) *J. Mol. Biol.* **130,** 103–134
16. Havas, K., Flaus, A., Phelan, M., Kingston, R., Wade, P. A., Lilley, D. M., and Owen-Hughes, T. (2000) *Cell* **103,** 1133–1142
17. Firman, K., and Szczelkun, M. D. (2000) *EMBO J.* **19,** 2094–2102
18. Petukhova, G., Van Komen, S., Vergano, S., Klein, H., and Sung, P. (1999) *J. Biol. Chem.* **274,** 29453–29462
19. Van Komen, S., Petukhova, G., Sigurdsson, S., Stratton, S., and Sung, P. (2000) *Mol. Cell.* **6,** 563–572
20. Ristic, D., Wyman, C., Paulusma, C., and Kanaar, R. (2001) *Proc. Natl. Acad. Sci. U. S. A.* **98,** 8454–8460
21. Saha, A., Wittmeyer, J., and Cairns, B. R. (2002) *Genes Dev.* **16,** 2120–2134
22. Yarranton, G. T., and Gefter, M. L. (1979) *Proc. Natl. Acad. Sci. U. S. A.* **76,** 1658–1662
23. Velankar, S. S., Soultanas, P., Dillingham, M. S., Subramanya, H. S., and Wigley, D. B. (1999) *Cell* **97,** 75–84
24. Dillingham, M. S., Wigley, D. B., and Webb, M. R. (2000) *Biochemistry* **39,** 205–212
25. Mazin, A. V., Zaitseva, E., Sung, P., and Kowalczykowski, S. C. (2000) *EMBO J.* **19,** 1148–1156
26. Guschin, D., Wade, P. A., Kikyo, N., and Wolffe, A. P. (2000) *Biochemistry* **39,** 5238–5245
27. Hamiche, A., Sandaltzopoulos, R., Gdula, D. A., and Wu, C. (1999) *Cell* **97,** 833–842
28. Jaskelioff, M., Gavin, I. M., Peterson, C. L., and Logie, C. (2000) *Mol. Cell. Biol.* **20,** 3058–3068
29. Langst, G., Bonte, E. J., Corona, D. F., and Becker, P. B. (1999) *Cell* **97,** 843–852
30. Whitehouse, I., Flaus, A., Cairns, B. R., White, M. F., Workman, J. L., and Owen-Hughes, T. (1999) *Nature* **400,** 784–787
31. Green, C. M., and Almouzni, G. (2002) *EMBO Rep.* **3,** 28–33
32. Peterson, C. L., and Workman, J. L. (2000) *Curr. Opin. Genet. Dev.* **10,** 187–192
33. Solinger, J. A., Lutz, G., Sugiyama, T., Kowalczykowski, S. C., and Heyer, W. D. (2001) *J. Mol. Biol.* **307,** 1207–1221
34. Solinger, J. A., and Heyer, W. D. (2001) *Proc. Natl. Acad. Sci. U. S. A.* **98,** 8447–8453
35. Alexiadis, V., and Kadonaga, J. T. (2002) *Genes Dev.* **16,** 2767–2771
36. Van Komen, S., Petukhova, G., Sigurdsson, S., and Sung, P. (2002) *J. Biol. Chem.* **277,** 43578–43587